

GVSPM for Reconstruction in Electrical Impedance Tomography

G. Y. Dong, H. Endo, *Student Member, IEEE*, S. Hayano, *Member, IEEE*, S. K. Gao, *Senior Member, IEEE*, and Y. Saito, *Member, IEEE*

Abstract—We apply the generalized vector sampled pattern matching (GVSPM) method to an inverse parameter problem for the reconstruction of electrical impedance tomography (EIT). Most of the inverse problems are reduced into solving for an ill-posed system of equations whose solution is not uniquely determined. The GVSPM introduced in this paper enables us to select the physically existing solution among possible ones. By applying GVSPM for EIT reconstruction, this point is verified by reliable reconstructed images.

Index Terms—Electrical impedance tomography (EIT), EIT reconstruction, finite volume method, generalized vector sampled pattern matching (GVSPM), sensitivity matrix method.

I. INTRODUCTION

ELECTRICAL impedance tomography (EIT) is reconstructing the conductivity distribution by the measured surface electrical potential distribution around the target when injecting current into the object. The surface electrical potential distribution generated by the injected current could be obtained as a solution of the Laplace equation. This leads EIT to a functional tomography depending on the medium parameter as well as boundary condition. This means that it is necessary to solve an inverse parameter problem for the realization of EIT which is difficult due to the ill-posed inverse problem. This is because boundary measurements are highly sensitive to a change in impedance near an electrode but far less sensitive to a central impedance change, meaning that large changes in conductivity may produce a small change in boundary voltage [1].

To obtain the normalized conductivity changes, we employ the generalized vector sampled pattern matching (GVSPM) method. The GVSPM method is an iterative solver for ill-posed linear system matrix, e.g., having a rectangular or singular matrix [2]. The key idea of the GVSPM is that the objective function is the angle obtained by means of the inner product between the input vector and solution of a system of equations. It has been successfully used for some applications, for example, current vector estimation from the locally measured magnetic field in cases of two-dimensional (2-D) and

quasi-three-dimensional (quasi-3-D) problems [2]–[5]. In this paper, the system matrix to be solved is constructed with normalized sensitivity matrix method [6] combining finite volume method (FVM) for the EIT forward problem [7].

II. GVSPM

Solving the inverse problems results in handling the ill-posed linear system of equations. The basic equation we have to solve is as follows:

$$\mathbf{Y} = \mathbf{C}\mathbf{X} \quad (1)$$

where \mathbf{Y} and \mathbf{X} denote the n th-order input and m th-order solution/output vectors, respectively, and \mathbf{C} is an n by m rectangular matrix. Equation (1) can be rewritten as

$$\mathbf{Y} = \sum_{i=1}^m x_i \mathbf{C}_i$$

$$\mathbf{X} = [x_1 \quad x_2 \quad \dots \quad x_m]^T, \quad \mathbf{C} = [\mathbf{C}_1 \quad \mathbf{C}_2 \quad \dots \quad \mathbf{C}_m]. \quad (2)$$

Equation (2) means that the input vector \mathbf{Y} is represented by means of a linear combination of column vectors \mathbf{C}_i , $i = 1, 2, \dots, m$, in the system matrix \mathbf{C} .

EIT is in essence to be reduced into solving the ill-posed system of (1). Therein, \mathbf{Y} and \mathbf{X} are the measured surface voltage vector with order n and solution vector of conductivity changes with order m , respectively, and \mathbf{C} is an n by m rectangular matrix, i.e., the sensitivity matrix in this paper.

A. Objective Function

Normalizing (2) by vector 2-norm $|\mathbf{Y}|$ gives the following relationship:

$$\frac{\mathbf{Y}}{|\mathbf{Y}|} = \sum_{i=1}^m x_i \frac{|\mathbf{C}_i|}{|\mathbf{Y}|} \frac{\mathbf{C}_i}{|\mathbf{C}_i|} \quad \text{or} \quad \mathbf{Y}' = \mathbf{C}'\mathbf{X}' \quad (3)$$

where the prime ($'$) denotes the normalized quantities.

Equation (3) means that the normalized input vector \mathbf{Y}' is obtained as a linear combination of the weighted solutions $x_i |\mathbf{C}_i| / |\mathbf{Y}|$, $i = 1, 2, \dots, m$, with the normalized column vectors $\mathbf{C}_i / |\mathbf{C}_i|$, $i = 1, 2, \dots, m$. It should be noted that the solution \mathbf{X} could be obtained when the inner product between \mathbf{Y}' and $\mathbf{C}'\mathbf{X}'$ becomes 1. This is the key idea of the GVSPM to construct the objective function f derived from the angle between the normalized input vector and output system of

Manuscript received June 18, 2002. This work was supported by the NSFC under Grant 59937160 and by the HBNSF under Grant 501037, P.R.C.

G. Y. Dong is with the Institute of Biomedical Engineering, Tsinghua University, Beijing, 100084, P.R.C. She is also with the Department of Electrical Engineering, Hebei University of Technology, Tianjin 300130, China (e-mail: dgy99@mails.tsinghua.edu.cn).

H. Endo, S. Hayano, and Y. Saito are with Graduate School of Engineering, Hosei University, Tokyo 184-8584, Japan (e-mail: endo@ysaitoh.k.hosei.ac.jp).

S. K. Gao is with Department of Electrical Engineering, Tsinghua University, Beijing 100084, China (e-mail: gsk-dea@tsinghua.edu.cn).

Digital Object Identifier 10.1109/TMAG.2003.810336

equations. When the objective function (4) reaches 1, the solution vector \mathbf{X} can be obtained as

$$f(\mathbf{X}^{(k)}) = \frac{\mathbf{Y}}{|\mathbf{Y}|} \cdot \frac{C\mathbf{X}^{(k)}}{|C\mathbf{X}^{(k)}|} = \mathbf{Y}' \cdot \frac{C'\mathbf{X}'^{(k)}}{|C'\mathbf{X}'^{(k)}|} \rightarrow 1. \quad (4)$$

B. Iteration Algorithm

Let $\mathbf{X}'^{(0)}$ be an initial solution vector given by

$$\mathbf{X}'^{(0)} = C'^T \mathbf{Y}'. \quad (5)$$

Then, the first deviation vector $\Delta\mathbf{Y}'^{(1)}$ is obtained as

$$\Delta\mathbf{Y}'^{(1)} = \mathbf{Y}' - \frac{C'\mathbf{X}'^{(0)}}{|C'\mathbf{X}'^{(0)}|}. \quad (6)$$

When the deviation $\Delta\mathbf{Y}'$ becomes a zero vector, the objective function (4) is automatically satisfied. Modification by the deviation vector $\Delta\mathbf{Y}'^{(k)}$ gives the k th iterative solution vector $\mathbf{X}'^{(k)}$, namely,

$$\begin{aligned} \mathbf{X}'^{(k)} &= \mathbf{X}'^{(k-1)} + C'^T \Delta\mathbf{Y}'^{(k)} \\ &= C'^T \mathbf{Y}' + \left(I_m - \frac{C'^T C'}{|C'\mathbf{X}'^{(k-1)}|} \right) \mathbf{X}'^{(k-1)} \end{aligned} \quad (7)$$

where I_m denotes an m by m unit matrix.

C. Convergence Condition

The convergence condition of the GVSPM iterative strategy is that the modulus of all characteristic values of the state transition matrix in (7) must be less than 1 [2]. The state transition matrix S is given by

$$S = I_m - \frac{C'^T C'}{|C'\mathbf{X}'^{(k-1)}|} = I_m - \frac{C'^T C'}{|\mathbf{Y}'^{(k-1)}|}. \quad (8)$$

Since the vector $\mathbf{Y}'^{(k-1)}$ is normalized, (8) can be rewritten as

$$S = I_m - C'^T C'. \quad (9)$$

Let λ be the characteristic value of the state transition matrix S . Then the determinant of symmetrical matrix is obtained as

$$|\lambda I_m - S| = \begin{vmatrix} \lambda & \varepsilon_{12} & \cdot & \varepsilon_{1m} \\ \varepsilon_{12} & \lambda & \cdot & \varepsilon_{2m} \\ \cdot & \cdot & \cdot & \cdot \\ \varepsilon_{1m} & \varepsilon_{2m} & \cdot & \lambda \end{vmatrix} = 0. \quad (10)$$

It is obvious that the modulus of off-diagonal elements in (10) is less than 1 because of the normalized column vectors of matrix C' , namely,

$$|\varepsilon_{ij}| < 1, \quad i = 1, 2, \dots, m, j = 1, 2, \dots, m. \quad (11)$$

Suppose that the modulus characteristic value $|\lambda|$ is more than 1; then the column vectors in (10) become linearly independent because of (11). In such a case, the determinant in (10) is not zero so that the condition $|\lambda| < 1$ should be satisfied. Therefore, it is proven that the GVSPM is always carried out on stable iteration.

III. EIT RECONSTRUCTION

A. Construction of a System Matrix

The construction of a system matrix is based on the normalized sensitivity matrix method [6] by combining FVM for the EIT forward problem [7], instead of the commonly used numerical method, the finite element method (FEM).

1) *FVM for the EIT Forward Problem*: The key idea of FVM is based on the current flow conservation law which satisfies the current continuity condition for current fields, i.e., the surface integral of the potential gradient in the presence of current sources in a control volume V with boundary surface S is given by the Gauss theorem

$$\oint_S (-\sigma \nabla \varphi) \cdot d\vec{S} = \iiint_V I_v dV \quad (12)$$

where σ , φ , and I_v are the conductivity, potential, and current volume source density in the control volume, respectively. In EIT, there is no current volume source I_v assumed in the bounded region. Thereby, (12) reduces to

$$\oint_S (-\sigma \nabla \varphi) \cdot d\vec{S} = 0. \quad (13)$$

The boundary conditions are given in

$$\begin{cases} -\sigma \frac{\partial \varphi}{\partial n} = J_n & \text{at the points where current is injected} \\ & \text{through the boundary } S \\ \sigma \frac{\partial \varphi}{\partial n} = 0 & \text{at the other points on } S \end{cases}$$

where J_n is the outward facing normal component of the current density.

Two kinds of mesh systems are needed for FVM which is the discretization of integral equation. For the 2-D case, the target region is divided into a large number of triangular elements which are called primary cells in FVM. In addition, complementary cells are also constructed by enclosing each of the nodes in order to calculate the current flow across each integration surface. The discretized equation is written as

$$\sum_i \int_{\Gamma_i} (-\sigma \nabla \varphi) \cdot d\vec{\Gamma}_i = 0. \quad (14)$$

The detailed description for the discretization is introduced in [7].

2) *Construction of a System Matrix*: The normalized sensitivity matrix method [6] is employed to construct the system matrix for reconstructing the normalized changes of conductivity in each element. The sensitivity matrix A and each individual boundary voltage measurement vector ΔV are normalized as C and ΔV_n in order to prevent its instability from measurement errors in practice. Therefore, the system matrix is the normalized sensitivity matrix C which describes the normalized linear sensitivity relationship between normalized changes in the boundary voltages ΔV_n and normalized conductivity changes in each element $\Delta\sigma_n$, as follows:

$$\Delta V_n = C \cdot \Delta\sigma_n. \quad (15)$$

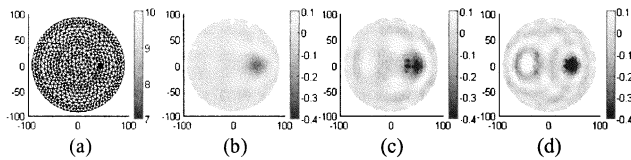


Fig. 1. Results for a single perturbation with conductivity change of 30% located 44 mm from the center of the circle. (a) Original conductivity distribution. (b) GVSPM result. (c) Pseudo-inverse result with truncation to 62 singular values. (d) Pseudo-inverse result with truncation to 78 singular values.

The simulated data ΔV_{sim} are constructed by subtracting the voltage boundary vector generated in uniform conductivity distribution from that generated in nonuniform conductivity distribution, instead of by multiplying a vector of conductivity changes $\Delta\sigma$ by sensitivity matrix A [8], so that the “inverse sin” problem is avoided.

B. Reconstruction Results

The physical model is a circle with a radius of 92 mm. A fine triangle mesh system containing 596 nodes and 1110 elements is shown in Fig. 1(a). The 96 measurement pairs are carried out with the opposite-adjacent measurement pattern. In this section, reconstructed images by both GVSPM and pseudo-inverse methods of system matrix are shown for comparison. Herein, the pseudo-inverse is carried out by the PINV routine in Matlab6.1 with the truncation level being set to 62 singular values. The truncation occurs at a value of about 0.03% relative to the maximum singular value of the system matrix.

1) *Performance for a Single Perturbation:* In this case, conductivity changes of 30% are defined in a small region containing six elements with the radius of about 6 mm, moving from the boundary to the center of the circle. Fig. 1 shows the original and calculated conductivity distribution when the perturbation is located 44 mm from the center of the circle.

For the case of a single perturbation, an image with high resolution and low localization error has been reconstructed in pseudo-inverse manner by using the pseudo-inverse routine of default tolerance, corresponding to the truncated level being set to 78 singular values of this system matrix, as shown in Fig. 1(d). However, the deficient side is that a pseudo image will also be produced symmetrically to the center against the image of the real perturbation. This will generate confusion with some other situations like the second case for two perturbations below, with two opposite conductivity changes of $\pm 30\%$. Even though the problem is improved by setting the truncated level to 62 singular values, shown in Fig. 1(c), comparing with the GVSPM result shown in Fig. 1(b), we can see that the image reconstructed by GVSPM performs more smoothly and more reliably. The localization error is within 2.5 mm when the distance between the perturbation and the center of the circle is over 30 mm. Because, for most of cases, more stable solutions can be obtained at the truncated level of 62 singular values than at 78 singular values for this system matrix, only the results reconstructed by pseudo-inverse at this truncation level to 62 singular values are shown and compared with the results by GVSPM in the following.

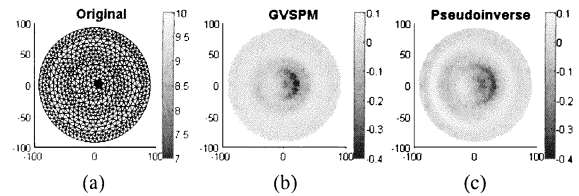


Fig. 2. The comparison with the perturbation located 5 mm from the center of the circle. (a) Original conductivity distribution. (b) GVSPM result. (c) Pseudo-inverse result.

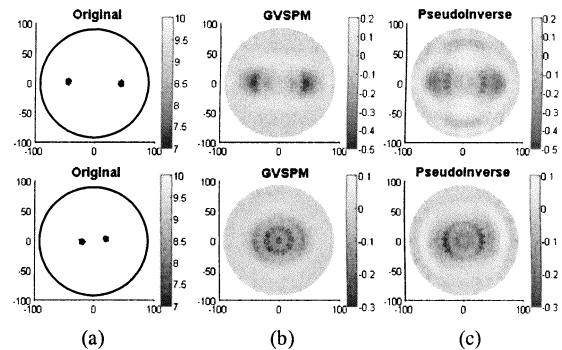


Fig. 3. Results with the two same conductivity changes of 30%, moving toward the center of the circle. (a) Original conductivity distribution. (b) GVSPM results. (c) Pseudo-inverse results.

With the perturbation moving toward the center within 10 mm, the image by GVSPM performs worse as well as that by the pseudo-inverse, shown in Fig. 2.

2) *Distinguishability With Two Perturbations:* Two cases are used in this session to check the distinguishability with two perturbations. In the first case, there are two small regions with the radii of about 6 mm symmetrical to the center of the circle, having the same conductivity changes of 30%. They are moved toward the center gradually along the diametral direction of the circle. In the second case, the opposite conductivity changes of $\pm 30\%$ are defined in the two small regions and moved the same way as the first case.

For the former case shown in Fig. 3, the images obtained by both GVSPM and the pseudo-inverse methods perform better toward the edge and worse toward the center. When their centers are less than 20 mm from the center of circle, respectively, the images are too blurred to distinguish them. However, for the latter case, shown in Fig. 4, the images obtained by two methods are of high resolution which is sufficient to be distinguishable, even when their centers are 10 mm from the center of the circle, respectively, as shown in the second row of Fig. 4.

Furthermore, comparing the results between GVSPM and pseudo-inverse methods, we can see that the qualities of reconstructed images by GVSPM are higher than those by the pseudo-inverse method. The images of perturbations are more shrunk and of less location errors, and the background is smoother.

3) *Performance of Sensitivity:* In order to know the sensitivity of conductivity changes, two perturbations with opposite conductivity changes of $\pm 1\%$ are defined in two regions with radii of about 6 mm, shown in Fig. 5(a). By combining FVM for the EIT forward problem with the normalized sensitivity matrix method for EIT reconstruction, images of relatively higher

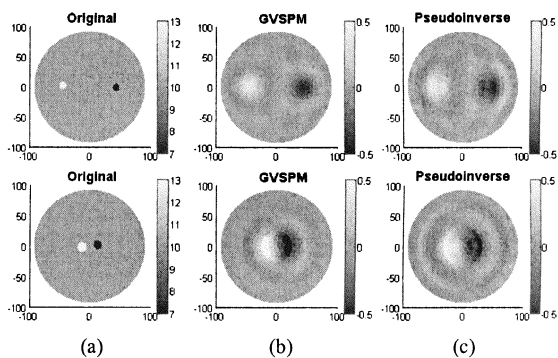


Fig. 4. Results with two opposite conductivity changes of 30%, moving toward the center of the circle. (a) Original conductivity distribution. (b) GVSPM results. (c) Pseudo-inverse results.

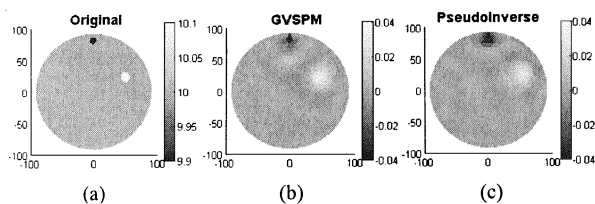


Fig. 5. The result with a change as small as 1%. (a) Original conductivity distribution. (b) GVSPM result. (c) Pseudo-inverse result.

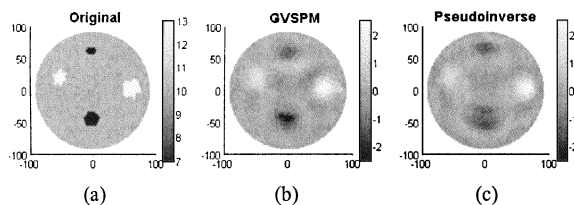


Fig. 6. The result with four perturbations. (a) Original conductivity distribution. (b) GVSPM result. (c) Pseudo-inverse result.

quality can be achieved by both GVSPM and pseudo-inverse methods, shown in Fig. 5(b) and (c), respectively.

Finally, we would like to show an example with four perturbations (see Fig. 6). Conductivity changes of -30% are defined in two regions located upside and downside of the circle, and the other two perturbations with conductivity changes of 30% are defined in two regions located at the left and right sides of the circle, respectively. Compared with the reconstructed image by the pseudo-inverse method, the image by GVSPM method is of more reasonable accuracy with higher resolution.

IV. CONCLUSION

We have succeeded in EIT reconstruction using the GVSPM method. Through comparison of the reconstructed images by GVSPM with those using the pseudo-inverse method, we know that the GVSPM images are of higher quality, i.e., the image of perturbation is more shrunk, has a higher resolution, and has less localization error. The background is reconstructed more smoothly which is useful for eliminating the confusion. A change as small as 1% can be distinguished by the GVSPM method as well.

However, one deficient side of GVSPM versus the pseudo-inverse method is that a longer computation time is needed for reconstructing the image. For this system matrix with 96 rows and 1110 columns, it takes about 8 min to make a cosine of the angle between the input vector and the vector of solution reach to 0.99999, with 1.4 GHz CPU and 1.5 Gbyte RAM.

As a result, GVSPM is a powerful iterative solver for any ill-posed linear system equations. It enables us to obtain reliable and stable solutions for EIT reconstruction and should be used in practice with experimental data in the near future.

REFERENCES

- [1] J.-P. Morucci and P.-M. Marsilli, "Bioelectrical impedance techniques in medicine, Part III: Impedance imaging, second section: Reconstruction algorithms," *Crit. Rev. Biomed. Eng.*, vol. 24, no. 4–6, pp. 599–671, 1996.
- [2] H. Endo *et al.*, "Generalized vector sampled pattern matching method—Theory and applications," in *Studies in Applied Electromagnetics and Mechanics*, F. Kojima *et al.*, Eds. Amsterdam, The Netherlands: IOS Press, 2002, vol. 23, Electromagnetic Nondestructive Evaluation (VI), pp. 285–292.
- [3] Sekijima, S. Miyahara, S. Hayano, and Y. Saito, "A study on the quasi-3D current estimation," *Trans. IEE Japan*, vol. 120-A, no. 10, pp. 907–912, 2000.
- [4] Y. Saito, E. Itagaki, and S. Hayano, "A formulation of the inverse problems in magnetostatic fields and its application to a source position searching of the human eye fields," *J. Appl. Phys.*, vol. 67, pp. 5830–5832, 1990.
- [5] K. Yoda, Y. Saito, and H. Sakamoto, "Dose optimization of proton and heavy ion therapy using generalized sampled pattern matching," in *Phys. Med. Biol.*, 1997, vol. 42, pp. 2411–2420.
- [6] P. Metherall, D. C. Barber, R. H. Smallwood, and B. H. Brown, "Three dimensional electrical impedance tomography," *Nature*, vol. 380, pp. 509–512, 1996.
- [7] G. Dong, X. Ma, S. Gao, Y. Xie, and Y. Saito, "Derivation from current density distribution to conductivities based on the adjoint field theory and numerical test with finite volume method," in *Proc. 2nd Japan-Australia-New Zealand Joint Seminar on Applications of Electromagnetic Phenomena in Electrical and Mechanical System (JANZS)*, Kanazawa, Japan, Jan. 24–25, 2002, pp. 89–96.
- [8] A. Liston, R. H. Bayford, A. T. Tidswell, and D. S. Holder, "A multi-shell algorithm to reconstruct EIT images of brain function," *Physiol. Meas.*, vol. 23, pp. 105–119, 2002.